

Enhancement of second-harmonic generation from metal nanoparticles by passive elements

Hannu Husu^{1,3}, Roope Siikanen¹, Robert Czaplicki¹, Jouni Mäkitalo¹,
Joonas Lehtolahti², Janne Laukkanen², Markku Kuittinen², and *Martti Kauranen¹

¹Department of Physics, Tampere University of Technology

P. O. Box 692, FI-33101 Tampere, Finland

Fax: + 358-3-31152600; email: martti.kauranen@tut.fi

²Department of Physics and Mathematics, University of Eastern Finland

P. O. Box 111, FI-80101 Joensuu, Finland

Fax: + 358-9-4512152; email: markku.kuittinen@uef.fi

³Centre for Metrology and Accreditation (MIKES)

P.O. Box 9, FI-02151 Espoo, Finland

Fax: + 358-10-6054299, hannu.husu@mikes.fi

Abstract

We prepare arrays of gold nanoparticles that include both noncentrosymmetric particles with a second-order nonlinear optical response and centrosymmetric particles with no second-order response. The latter particles act as passive elements that modify the electromagnetic mode structure of the sample and enhance second-harmonic generation from the active particles.

1. Introduction

Antennas are components that enable the coupling of electromagnetic radiation from a source into the far field or vice versa [1, 2]. Recent advances in nanofabrication have allowed antenna concepts to be moved from the radio-frequency to the optical domain, with several impressive demonstrations [3]. Passive elements play an important role in the design of antennas. They are used to improve the directionality or other properties of the antennas.

In this Paper, we bring the concept of passive elements to the field of nonlinear metamaterials consisting of plasmonic metal nanoparticles. We prepare arrays of nanoparticles that combine both noncentrosymmetric L-shaped particles and centrosymmetric bars. The former act as metamolecules with a second-order nonlinear optical response, whereas the latter act as passive elements with no second-order response. The presence of the passive elements is shown to enhance the efficiency of second-harmonic generation (SHG) compared to a similar sample without passive elements.

2. Samples and experiments

Arrays of gold nanoparticles were prepared by electron-beam lithography and lift-off. The SHG-active particles are L-shaped [4] with the linewidth of 100 nm and arm length of either 175 nm or 275 nm. The shape is strongly dichroic with eigenpolarizations along the shape symmetry axis (y) and orthogonal to that (x). The antenna particles are bars with the linewidth of 50 nm and length 300 nm. All particles are 20 nm thick and there is a thin adhesion layer of chromium between the gold and silica substrate. The particles are also covered by a 20 nm thick protective layer of silica. SEM images of the samples are shown in Fig. 1.

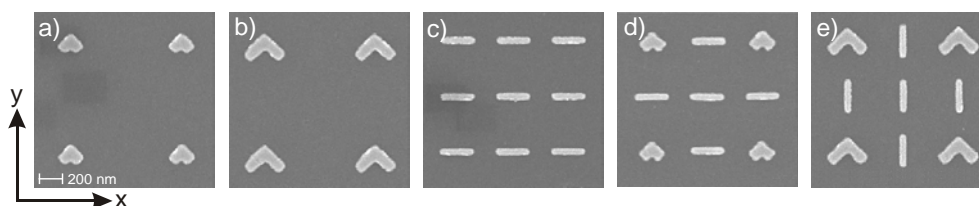


Fig. 1: SEM micrographs of the samples. a) L's with 175 nm arm length; b) L's with 275 nm arm length; c) Bars with 300 nm length; d) L's with 175 nm arm length and bars in x orientation; e) L's with 275 nm arm length and bars in y orientation. The coordinate system for the samples is also shown.

The two-dimensional arrays had an underlying square lattice with 500 nm period. The SHG-active reference samples consisted of only L's in an array of 1000 nm period (Fig. 1a,b). The passive reference samples consisted of only bars at each lattice point (Fig. 1c). Finally, the samples combining L's and bars included the L's in the original positions, whereas the bars were placed in the remaining lattice points and they were oriented either along the x or y direction (Fig. 1d,e).

The extinction spectra of the samples were measured at normal incidence using linearly polarized light and fiber-optic spectrometers. Combining the results from two spectrometers allowed the spectra to be recorded over the wavelength range 400-1700 nm.

SHG measurements were performed with an Nd:glass laser (1060 nm, 200 fs, 80 mW, 82 MHz) at normal incidence and essentially collimated and linearly-polarized light (Fig. 2). The structure of the sample dictates that the nonvanishing signals correspond to the tensor components yyy and yxx , where the first letter refers to the detected polarization component of SHG light and the two last letters refer to the polarization of the fundamental field. Note that the symmetry would allow also the signal $xyx=xyx$, but these components cannot be addressed individually. The linear polarization of fundamental light was controlled by calcite Glan polarizer and half-wave plate (HWP). The detected SHG polarization was selected by a Glan polarizer. A visible blocking filter was placed before the sample to filter out second-harmonic signal from the polarization optics and an infrared blocking filter was placed after the sample to block the fundamental laser beam. The second-order response was determined from the quadratic dependence of the SHG intensity on the fundamental intensity. It was measured with a photomultiplier tube (PMT) combined with a photon counting unit for sensitive light detection.

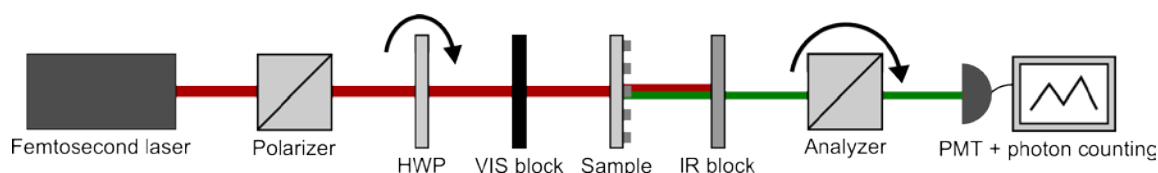


Fig. 2: Setup for second-harmonic measurements.

3. Results

The extinction spectra of the samples are shown in Fig. 3. The L samples exhibit a short-wavelength resonance for y polarization and a long-wavelength resonance for x polarization (Fig 3a,b). For the larger (smaller) particles the former (latter) is close to our laser wavelength. The bars exhibit a plasmon resonance related to the long axis at 1450 nm (Fig. 3c), relatively far from the laser wavelength.

For the samples with L's and bars, the long axis of the bars was chosen in the direction corresponding to the eigenpolarization of the L near the laser wavelength. For both large and small L's, the spectra are seen to be modified more than a mere superposition of the L and bar spectra even though the resonance of the bar is relatively far from the respective resonance of the L (Fig. 3d,e). In particular, the spectra at the laser wavelength are enhanced compared to the L-only samples.

The SHG signal levels of the samples are shown in Table 1. For the L reference samples, the strongest signals correspond to the tensor component for which the polarization of the fundamental wavelength is reso-

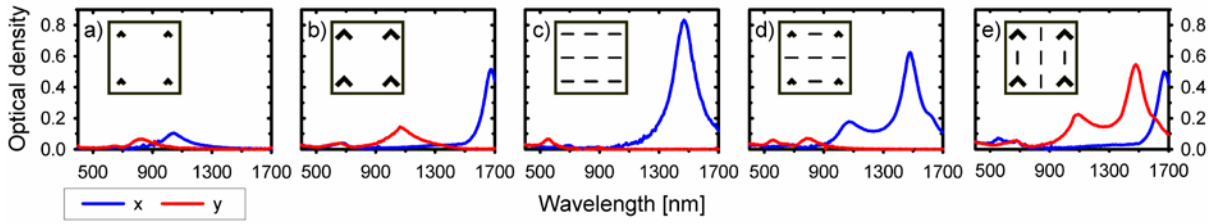
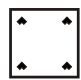
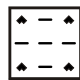




Fig. 3: Polarized extinction spectra of the samples. a) L-shapes with 175 arm length; b) L-shapes with 275 arm length; c) Bars with 300 length; d) L-shaped particles with 175 arm length and bars in x orientation; e) L-shaped particles with 275 arm length and bars in y orientation.

nant with the particles [5]. The SHG signals from the bars only were several orders of magnitude lower in agreement with their centrosymmetric structure.

When the L's and bars are combined, the strongest SHG signals are seen to be enhanced by about a factor of two compared to the respective reference sample. This suggests that the enhancement is related to the modification of the plasmon resonances at the fundamental wavelength and associated local-field distributions affected by the passive bars. This result is further supported by the fact that the effect of bars oriented in the orthogonal direction had very little effect on the SHG signals (data not shown).

Table 1: SHG signals from the various samples

reference sample	tensor component		actual sample	tensor component	
	yyy	yxx		yyy	yxx
a 	2	1118	d 	6	2247
b 	682	54	e 	1514	34

4. Conclusions

We have shown that second-harmonic generation from arrays of noncentrosymmetric metal nanoparticles can be enhanced by using additional passive elements, which are centrosymmetric, in the array. In the present first demonstration of this concept, the passive elements were found to modify the electromagnetic properties of the sample at the fundamental wavelength. A factor of two enhancement was obtained, although the plasmon resonances of the active and passive particles occurred at relatively different wavelengths. There is thus a lot of room for further optimization. In the future, it will also be interesting to use passive elements to aid the coupling of second-harmonic radiation out of the sample.

References

- [1] P. Muhlschlegel, H.-J. Eisler, O. J. F. Martin, B. Hecht, and D. W. Pohl, Resonant optical antennas, *Science*, vol. 308, no. 5728, pp. 1607-1609, 2005.
- [2] L. Novotny and N. van Hulst, Antennas for light, *Nat. Photon.*, vol. 5, no. 2, pp. 83-90, 2011.
- [3] P. Biagioni, J.-S. Huang and B. Hecht, Nanoantennas for visible and infrared radiation, *Reports on Progress in Physics*, vol. 75, no. 2, pp. 024402, 2012.
- [4] R. Czaplicki, M. Zdanowicz, K. Koskinen, J. Laukkanen, M. Kuittinen and M. Kauranen, Dipole limit in second-harmonic generation from arrays of gold nanoparticles, *Opt. Express*, vol. 19, no. 27, pp. 26866-26871, 2011.
- [5] F. B. P. Niesler, N. Feth, S. Linden and M. Wegener, Second-harmonic optical spectroscopy on split-ring-resonator arrays, *Opt. Lett.*, vol. 36, no. 9, pp. 1533-1535, 2011.